https://doi.org/10.5194/egusphere-2026-2062
Preprint. Discussion started: 21 April 2026

First Energetic Neutral Atom images of the Earth's magnetosphere from the JENI detector on board the JUICE mission during the Lunar and Earth Gravity Assist

Konstantinos Dialynas[1,13], Matina Gkioulidou[2,13], Donald G. Mitchell[2], Pontus C. Brandt[2], George Clark[2], Elias Roussos[3], Peter Kollmann[2], Leonardo Regoli[2], Frederic Allegrini[4,5], Nicolas Andre[6,7], Xianzhe Jia[8], Krishan Khurana[9], Carol Paty[10], Stas Barabash[11], Peter Wurz[12]

[1]Academy of Athens, Center for Space Research and Technology, Athens, Greece

[2]Johns Hopkins Applied Physics Laboratory, Laurel, MD, USA

[3]Max Planck Institute for Solar System Research

[4]Southwest Research Institute, San Antonio, TX

[5]Department of Physics and Astronomy, University of Texas at San Antonio, San Antonio, Texas, USA

[6]Institut de Recherche en Astrophysique et Planétologie (IRAP), CNES-CNRS-Université Toulouse III Paul Sabatier, Toulouse, France

[7]Institut Supérieur de l'Aéronautique et de l'Espace (ISAE-SUPAERO), Université de Toulouse, Toulouse, France

[8]Climate and Space Sciences and Engineering, University of Michigan, USA

[9]Department of Earth, Planetary and Space Sciences, University of California at Los Angles, Los Angeles, CA90095, USA

[10]Department of Earth Sciences, University of Oregon, 100 Cascade Hall, Eugene, OR 97403-1272, USA

[11]Sweedish Institute of Space Physics, Kiruna, Sweeden

[12]Space Science and Planetology, Physics Institute, University of Bern, Bern, Switzerland

[13]K. Dialynas and M. Gkioulidou contributed equally to this work.

Correspondence to: Konstantinos Dialynas (kdialynas@phys.uoa.gr)

https://doi.org/10.5194/egusphere-2026-2062
Preprint. Discussion started: 21 April 2026

Abstract. The Jovian Energetic Neutrals and Ions (JENI), part of the Particle Environment Package (PEP), on the Jupiter Icy Moons Explorer (JUICE) spacecraft is a state-of-the-art detector, capable of analyzing the energy and direction of incident Energetic Neutral Atoms (ENAs) from planetary magnetospheres. Our analysis focuses on 2.86-85.5 keV Hydrogen ENA measurements between 21 to 24 August 2024 when JUICE performed the Lunar and Earth Gravity Assist (LEGA). During the LEGA, JENI had a unique opportunity to obtain continuous, 7.5-minute accumulation time global images of the terrestrial magnetosphere as the spacecraft moved outward from ~17 to 150 Earth Radii. Although there were no indications of substantial geomagnetic storms developing during that time, substorm activity was observed based on eight distinct dips of the SuperMAG AL (SML) index down to ~-250 nT for the four last ones and even down to ~-400 nT for the four first ones. Our results indicate increased ENA emissions associated with the onsets of these events, suggesting direct responses to the increased energetic ion activity during those substorm events. Unlike the periods of intense geomagnetic storms, during which proton intensities build up the ring current evolving from an asymmetric distribution during the main phase to a roughly symmetric distribution during the recovery phase, the images from JENI during this interval show non-uniform ENA emissions in the plasma sheet, suggesting transient processes, such as a series of repeated nightside injections. The nightside ENA intensities are generally brighter than those from the dayside, possibly reflecting magnetotail processes associated with energetic ions being injected.

1 Introduction

Energetic neutral atom (ENA) imaging has emerged over the years as a powerful means to diagnose the global, underlying ion distributions of the terrestrial magnetosphere (e.g. Brandt et al. 2021; 2022) and the magnetospheres of the outer planets together with moons exospheres (e.g. Krimigis et al. 2002, Mauk et al., 2003, 2004; Mitchell et al., 2004, Barabash et al., 2006; 2007, Orsini et al., 2010, Brandt et al., 2008; 2010; 2012, Dialynas et al. 2013). As a magnetically trapped ion in the magnetosphere exchanges charge with a stable, cold neutral particle, the ion is thereby neutralized and becomes an ENA. Sufficiently energetic ENAs, i.e. exceeding their escape energies (e.g. E>1 eV at Earth) travel in straight lines from their origin, maintaining their direction, energy, and species. Thus, ENA imaging provides global images of the underlying plasma distributions together with valuable compositional and spectral information, being the only technique capable of imaging the dynamics of the ion population over large parts of a magnetosphere simultaneously, e.g. the Earth's plasma sheet and ring current.

From reconstructed ENA images based on IMP-7/8 measurements (e.g. Roelof et al. 1985) to the first ENA images of the terrestrial ring current from MEPI/ISSE-1 (e.g. Roelof, 1989), or subsequent ones from Cassini/INCA in 1997 (e.g. Krimigis et al. 2004) and the Low Altitude Emissions from Astrid (e.g. Brandt et al., 1997), the modern ENA cameras, like the Imager for Magnetopause-to-Aurora Global Exploration (IMAGE; Burch, 2000) and the Two Wide angle Imaging Neutral-atom Spectrometers (TWINS; McComas et al. 2009), have provided detailed ENA observations of the plasmasheet (e.g. Brandt et al. 2002) and the global state of the ring current during geomagnetic storms (Mitchell et al. 2003).

https://doi.org/10.5194/egusphere-2026-2062
Preprint. Discussion started: 21 April 2026

Substorm injections have been observed with the IMAGE/HENA ENA camera [Brandt 2021; Mitchell 2003]. However, HENA's spin duty cycle and low sensitivity only allowed for tens of minutes time-averaged measurements. Keesee et al. (2021) used TWINS ENA data to develop ~3-min averaged (i.e., during 2 sweeps of the actuator that rotates to provide the second spatial dimension) "effective" temperature maps. They presented localized regions of increased ion temperature by projecting the pixels to the magnetic equator. Those regions were associated with a dipolarization front with bursty ion flows measured by the in-situ MMS mission (Burch et al. 2016). However, due to low sensitivity of the ENA camera onboard TWINS (due to very small geometric factor and duty cycle; McComas et al. 2009), only limited energies can be used (2–32 keV), assuming Maxwellian distribution, to retrieve those temperatures.

Injections at Earth are a complex phenomenon, but the storm-time vs non storm-time cases exhibit some clear signatures in particle dynamics that can easily be identified in ENA images. In brief, storm-time substorms include a gradual increase of hydrogen ENA intensities in both the plasmasheet and the ring current, together with a very sudden intensification of oxygen ENAs related to non-adiabatic acceleration of ions during rapid magnetic field reconfigurations (e.g. Mitchell et al. 2003). Similar characteristics have been reported at Saturn using Cassini measurements (e.g. Mitchell et al. 2005, Dialynas et al. 2009). Injection events that are not related to geomagnetic storms show weak, or no intensification of oxygen ENAs due to the lack of significant amounts of singly ionized oxygen in the plasma sheet (e.g. Nose et al. 2010). Whatever the mechanism responsible for plasma transport and acceleration in the magnetosphere, the injections occur consistently with substorm auroral activity (e.g. Liou et al. 2000).

In the present analysis we employ Hydrogen ENA observations from the Jovian Energetic Neutrals and Ions (JENI) instrument on the Jupiter Icy Moons Explorer (JUICE) spacecraft to discuss substorm dynamics of the ENA emissions around Earth from vantage points much further away from the Earth than any other previous mission. Section 2 describes the measurement techniques, Section 3 describes our analysis of the measured ENAs, whereas sections 4 and 5 provide a short discussion of our results and a short summary, respectively.

2 The Jovian Energetic Neutrals and Ions (JENI) Instrument

We use ENA measurements from the Jovian Energetic Neutrals and Ions (JENI) instrument (Mitchell et al. 2016), part of the Particle Environment Package (PEP) suite on board the Jupiter Icy Moons Explorer (JUICE) mission to Jupiter. JENI is a combined ENA and ion detector with a large field of view (≥92°x120.6°) that builds on the heritage of the High-Energy Neutral Atom (HENA) camera (Mitchell et al. 2000) on board the IMAGE mission and the Ion and Neutral Camera (INCA) on the Cassini spacecraft (Krimigis et al. 2004) that operated between 1997 to 2017, and it is almost an identical copy to the IMAP-Ultra detector (Gkioulidou et al. 2026), taking high signal-to-noise images of Energetic Neutral Atoms (ENAs).

JENI is capable of alternating between ion and ENA modes. During the observation period analyzed here, JENI was operated in ENA mode, where its thin conductive plates were held at a relatively low voltage about 1 kV deflecting charged

https://doi.org/10.5194/egusphere-2026-2062
Preprint. Discussion started: 21 April 2026

particles up to about 20 keV/q, but will be run at a higher voltage during its prime mission at Jupiter. A variable aperture slit can accommodate different geometric factors (0.001 - 1.85 cm^2 sr) and effectively filter Ultraviolet (UV) light when the Sun is in the detector's field of view (FOV). The detector can analyze separately the gross composition, velocity and direction of the incident ENAs, based on the time-of-flight (TOF) technique and defines several energy channels within the energy range of ~1 to ~110 keV. The nominal angular resolution of JENI is ~10° FWHM at ~5 keV incident energy for hydrogen, ~10° at ~20 keV incident energy for Oxygen (~20° at 10 keV total energy), but can be energy dependent, increasing toward lower energies. More details about JENI can be found in Brandt et al. (2026).

3 Energetic Neutral Atom Observations

In order to direct its trajectory towards Venus, the JUICE spacecraft performed the so-called Lunar and Earth Gravity Assist (LEGA) during the time period between 19 and 23 August 2024. As depicted in the left panel of Figure 1, the spacecraft entered Earth's magnetosphere from the tail and approached Earth at 21:16 UTC on 19 August 2024. At the outbound leg of this trajectory, between 21 August 2024 (~00:15 UTC) and 23 August 2024 (~22:50 UTC) JENI was set to ENA mode, providing remote observations of the terrestrial environment (middle and right panels of Figure 1).

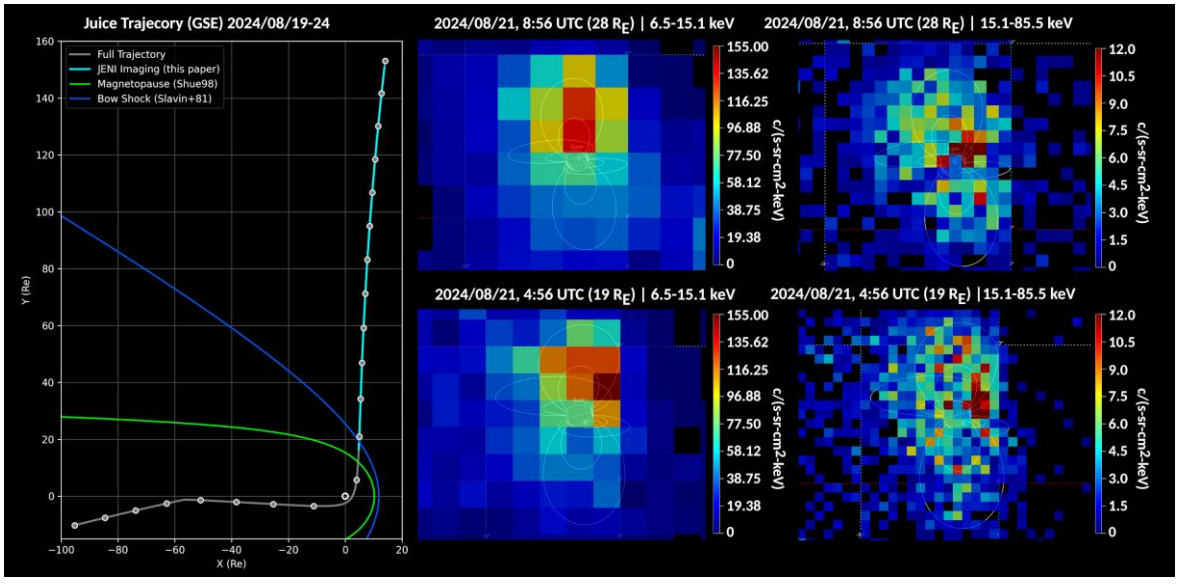

Figure 1: (left) The trajectory of JUICE between 19 and 24 August 2024 in the Geocentric Solar Ecliptic (GSE) coordinate system, in which the X-axis is pointing towards the Sun, the Z-axis points toward north (perpendicular to the ecliptic plane), and the Y-axis completes the right hand system, pointing towards dusk. In this projection, JUICE approaches from the left. A small trajectory deflection is observed at the moon flyby. Markers along the trajectory are spaced every 6h. (Middle) Characteristic, 7.5-minute accumulation time, high energy resolution images of 6.5-15.1 keV ENAs from JENI, after JUICE crossed the magnetopause. The Earth is shown in the middle of these images, whereas its dipole L-shell lines at L=4 and L=8 at local times 00:00, 06:00, 12:00, and 18:00 are also included for reference. (Right) The corresponding high angular resolution images of 15.1-85.5 keV ENAs from JENI. In both data plots, the flipped appearance of the Earth's magnetosphere is due to the projection of the observations in the instrument frame.1.1.2 Equations

https://doi.org/10.5194/egusphere-2026-2062
Preprint. Discussion started: 21 April 2026

During the time period where JENI was set to ENA mode, JUICE was surveying the equatorial plane and traveling away from Earth, through a radial distance of about 17 R_E and beyond, resulting in a series of more than 500 continuous 7.5-minute accumulation time images up to ~150 RE (1 R_E ~ 6,378 km). The images in the right panels of Figure 1 provide first observations from JENI regarding the variation in the Hydrogen ENA emission from the terrestrial ring current and plasmasheet. The bright, predominantly night-side emission in Figure 1, where JUICE was close to Earth at ~19 R_E is slightly diminished about 4 hours later, as it moved further away by ~9 R_E. The fainter emissions from dayside exhibit a similar variability, although they look less prominent. These images can be considered to be representative of the Hydrogen ENA emissions around Earth beyond~ 6.5 keV.

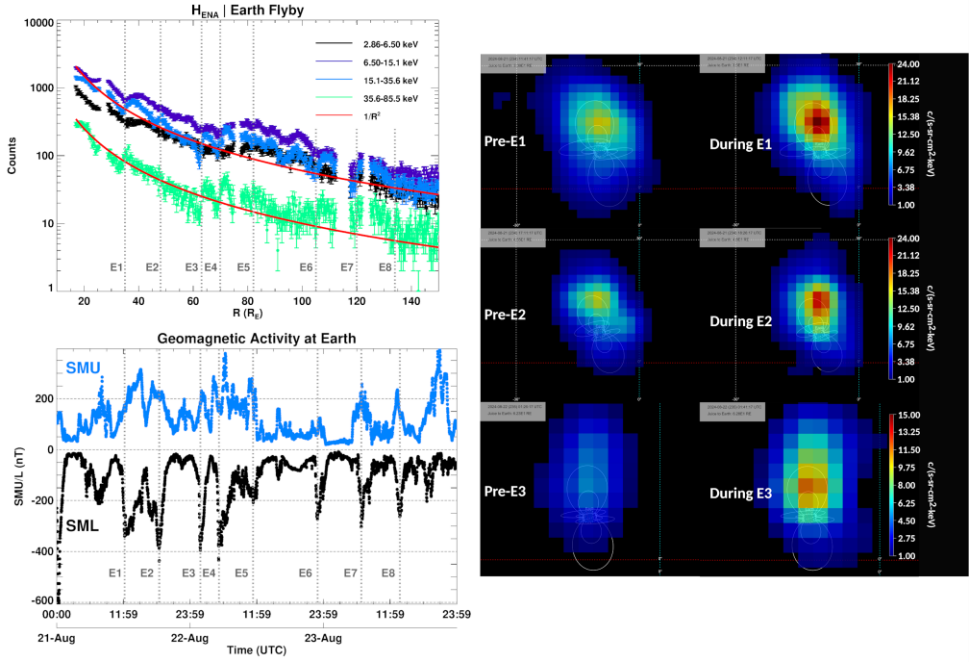

Figure 2: (top left) Hydrogen ENA counts for different energies between 2.86 and 85.5 keV, summed over selected pixels around Earth that include the entire magnetosphere (both the dayside and nightside) and plotted as a function of JUICE's distance to Earth. Each datapoint corresponds to a 7.5-minute accumulation time image. The R^{-2} lines (red lines) are drawn for reference, whereas the gray lines indicate events of increased geomagnetic activity according to the SML index. (bottom left) One minute resolution SMU and SML indices provided by the SuperMAG collaborators (Newell and Gjerloev 2011) that correspond to JENI's observation period (21 to 24 August 2024) plotted as a function of time. The time periods where SML suggests substorm activity are indicated with dashed gray lines. (Right) A series of 7.5-minute accumulation time, 15.1-35.6 keV Hydrogen ENA images before and during the periods of increased geomagnetic activity, slightly smoothed to aid interpretations.

https://doi.org/10.5194/egusphere-2026-2062
Preprint. Discussion started: 21 April 2026

Figure 2 provides a more comprehensive view of the variability of the ENA emissions from Earth during the LEGA. The summed counts in the top left panel of Figure 2 indicate that the 2.86-85.5 keV ENA emissions are decreasing with increasing spacecraft distance. Notably, the overall ENA signal strength falls off as the spacecraft moves away from the ENA source roughly following a R^{-2} line (e.g. Mitchell et al., 2004). However, as clearly shown in Figure 2, the rough R^{-2} trend is interrupted by slight enhancements (Ei, i=1-8) in the total counts, apparent throughout the 2.86-85.5 keV energy range (although the changes in the 2.86-6.5 keV channel are somewhat less pronounced) which roughly coincide with the time periods where the SuperMAG AL (SML) index (e.g. Newell and Gjerloev 2011), a generalization of the AL index capturing the magnitude of substorms (bottom left panel in Figure 2), is minimum. In fact, the histories of total ENA counts around Earth shown in the top panel of Figure 2 reveal enhancements up to at least 135 R_E.

Albeit the interplanetary magnetic field (IMF) did not display any noteworthy magnitude and/or direction changes and there were no indications of any substantial geomagnetic storm developing during the time period where JENI was imaging the terrestrial magnetosphere, the SML index shows clear substorm activity. While ENAs are considered to be long distance communicators of the processes that their parent ion distributions undergo, we conclude that these increased ENA emissions are a direct response to the increased energetic ion activity during those substorm events. The series of 15.1-35.6 keV Hydrogen ENA images in the right panel of Figure 2 further corroborate this conclusion, showing that ENA emissions around Earth broaden and increase in intensity during each substorm event (here we only focused on the three first substorm events, E1-E3).

Studying the terrestrial plasma sheet (or the ring current) with ENA images requires excluding pixels that can be attributed to LAEs. LAEs are due to mirroring ions that undergo charge exchange with the ambient singly ionized oxygen at the top layers of the terrestrial atmosphere (e.g. Roelof 1997, Brandt et al. 2001, Goldstein et al. 2018) and can substantially dominate the ENA emissions compared to those from the plasmasheet. To roughly differentiate between ENAs that are due to Low Altitude Emissions (LAE) and those that originate from the plasmasheet, Figure 3 shows the intensities of 2.86 - 85.5 keV ENAs using selected pixels from the dayside and the nightside, away from Earth.

Clearly, the nightside plasmasheet is more pronounced and the ENA flux decay is somewhat less steep as a function of distance than the ENA flux associated with the dayside. Most importantly, unlike the dayside ENA intensities that keep decreasing, the ENA flux on the nightside increases right after the E1 event. This suggests that we are likely looking at transient processes, such as a series of repeated nightside injections that are not necessarily related to a global process, e.g. a global geomagnetic storm, where the Hydrogen ENA flux would be enhanced nearly symmetrically around Earth, with associated O^+ enhancements in the ring current region (e.g. Daglis, 1997; Daglis et al., 1999, Mitchell, et al., 2003).

https://doi.org/10.5194/egusphere-2026-2062
Preprint. Discussion started: 21 April 2026

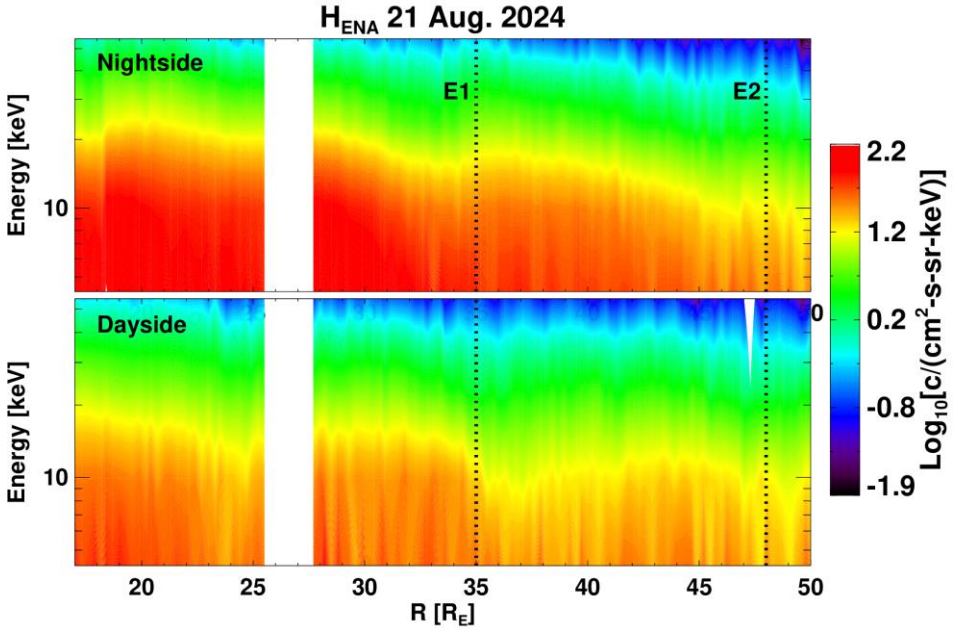

Figure 3: Color coded ENA flux as a function of distance produced by averaging, high energy resolution, 2.86-85.5 keV Hydrogen ENA intensities over selected pixels from the (top) nightside and (bottom) dayside magnetosphere, avoiding pixels close to Earth that could be attributed to Low Altitude Emissions (LAE). The spectrogram is slightly smoothed in the energy-direction to enhance visibility. As JUICE moves away from Earth, the process of avoiding pixels including LAEs becomes increasingly difficult and the ENAs from the plasmasheet can be fairly resolved up to ~50 R_E, and this is why E3 (>60 R_E) is not plotted here. The use of high angular resolution images would extend this range to longer distances, but would not allow resolving the energies in four discrete energy channels between 2.86-85.5 keV, as shown here. The dashed black lines correspond to the first two substorm events identified via the SML index in Figure 2. During the imaging period, the voltage at JENI's deflection plates was set to relatively low values, i.e. ~1.0 kV, but was adequate to sweep out protons from the detector up to about 20 keV. Given that JUICE is mostly outside Earth's magnetosphere, the foreground ion intensities are substantially lower than the ENA intensities.

A closer investigation of the ENA enhancements for E1 is shown in Figure 4 (E2 and beyond show similar signatures). The image on the top left panel of Figure 4 (12:03 UTC) exhibits relatively enhanced ENA emissions close to Earth, roughly around the L=8 line, followed by a large intensification of the night side emissions (13:03 UTC) consistent with E1 identified in Figure 2. The ENA emissions on the nightside remain high beyond about 2 hrs (15:11 UTC) after the onset of E1. The dayside ENA emissions do not show the same variability as the nightside, but remain nearly constant throughout the E1 event.

https://doi.org/10.5194/egusphere-2026-2062
Preprint. Discussion started: 21 April 2026

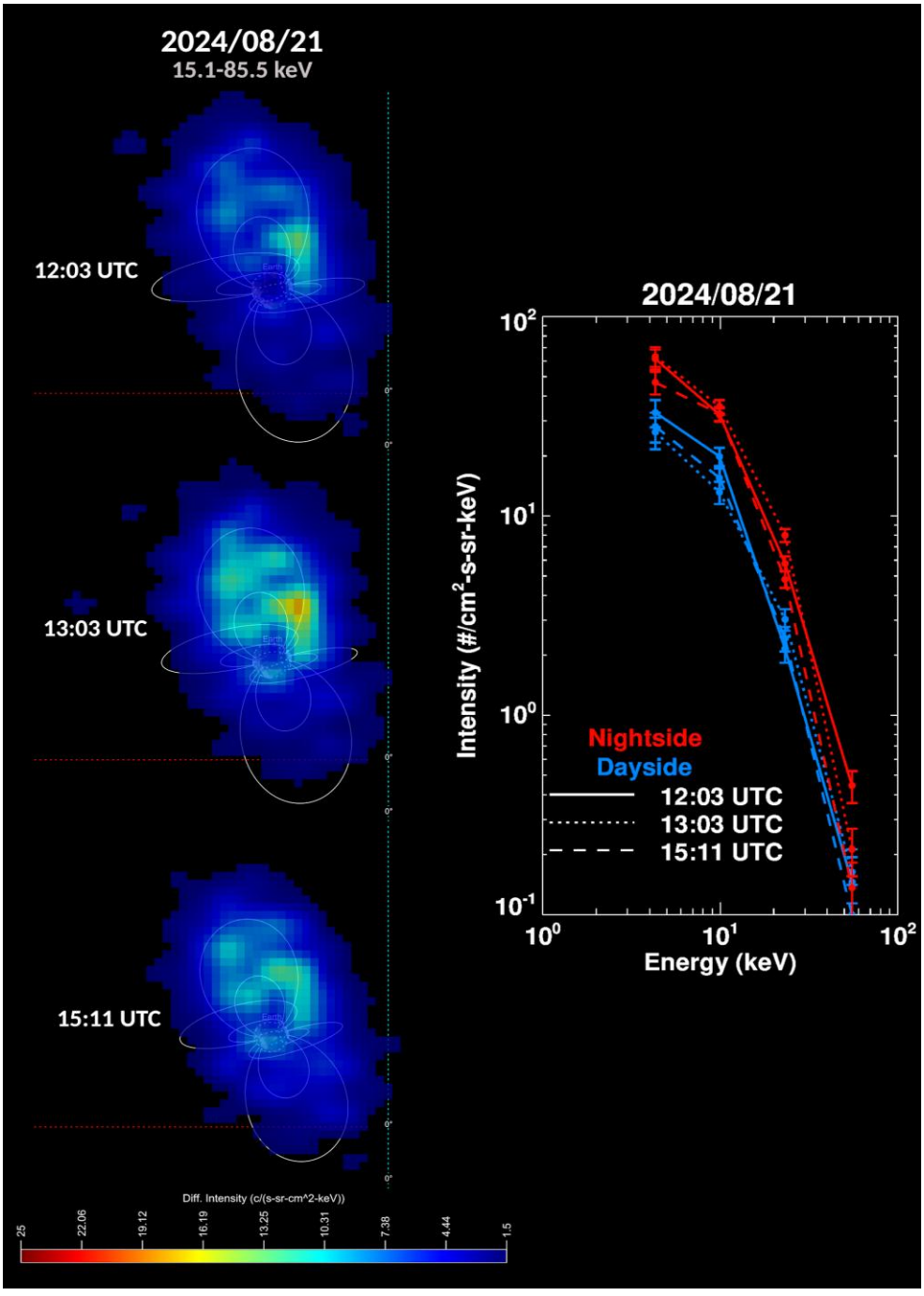

Figure 4. (left) A series of 82.5-minute accumulation time, 15.1 - 85.5 keV high angular resolution images of Hydrogen ENAs (top) right before E1 (middle) right after E1 and (bottom) as E1 progresses (details about E1 and other events are shown in Figure 2). The images are slightly smoothed to better aid interpretations. (right) The corresponding energy spectra of 2.86-85.5 keV Hydrogen ENAs from the measurements shown in Figure 3.

https://doi.org/10.5194/egusphere-2026-2062
Preprint. Discussion started: 21 April 2026

These characteristics are very consistent to other "non-storm" time injection events identified previously by the IMAGE/HENA at Earth (e.g. Brandt P. C. 2021). In addition to the nightside enhancements, the images after the onset of E1 show a distinct enhancement in ENA intensities at low altitudes (compared to the one before E1), possibly indicative of LAEs. While particles of ~10 keV to a few 100s of keV dominate most of the total current density (e.g. Daglis et al., 1999), it is possible that a fraction of the same particles injected from the plasma sheet forming the ring current are charge exchanging and being lost as LAEs (e.g. Mackler et al. 2016). However, our preliminary analysis of these ENA emissions cannot resolve these effects and conclude whether these low altitude ENA enhancements are a direct response to the E1. Such questions can be addressed via forward models or other inversion techniques (e.g. Roelof and Skinner 2000; DeMajistre et al. 2004; Brandt et al. 2022), a task that would be performed in a future analysis.

The 2.86-85.5 keV ENA intensities deviate from a standard power law form in energy (Right panel in Figure 4). The ENA energy spectra seem to develop a slight roll off below ~6.5 keV. Albeit the nightside intensities are persistently higher than those from the dayside, we do not observe changes in the slopes or the peaks of the distributions, at least not for the ENA energy spectra surrounding E1. Notably, most of the change between the pre and post-event spectra occurs at energies between 6.5 keV and 55 keV whereas the higher energy ENA intensities are higher before the E1 event. Although this may be part of the standard ENA intensity variation/fluctuation at this energy, it is also not inconsistent with the fact that during injections, ions with energies below about a few tens of keV contribute more significantly to the ring current and plasma sheet than those with higher energies (e.g. >100 keV). Higher-energy protons usually dominate during quiet times, and although not specific to our analysis- also during the recovery phase following a geomagnetic storm (e.g. Gkioulidou et al. 2016). However, it is still puzzling why the 35.6-85.5 keV channel is low in intensities during the event.

4 Discussion

Our analysis indicates that the overall morphology of the 2.86-85.5 keV ENA emissions during LEGA is not consistent with a global process, such as a global geomagnetic storm, but transient processes, such as a series of repeated nightside injections. This is further corroborated by the fact that during the LEGA there are no indications of a storm, but only changes in the SML index that point toward non-storm injections from substorm auroral activity. The correlation between ENA and the non-storm time substorm activity has been documented before (e.g. Brandt et al. 2018 and references therein), not only for Earth, but also Saturn (e.g. Mitchell et al. 2005). Apparently, even localized magnetospheric processes, such as the nightside injections, produce pressure driven currents that trigger the aurora, and ENA imaging is a very efficient way to capture the dynamics of the system.

There are still two issues concerning our results, requiring further analysis in the future. The first is that the low energy ENA channel (2.86-6.5 keV) is less responsive to the injection events than higher energies (6.5-85.5 keV). For example, although the 2.86-6.5 keV ENA emissions increase after each nightside injection episode, they do so with a slight

https://doi.org/10.5194/egusphere-2026-2062
Preprint. Discussion started: 21 April 2026

time lag (e.g Figure 1). This may be due to the fact that the total current density at Earth's plasmasheet is dominated by particles of ~10 keV to a few 100s of keV (e.g. Daglis et al., 1999). The second issue is that between E5 and E6 we see ENA enhancements which may correspond to a very small change in the SML index, meaning that ENA variability at Earth is complex and may not be uniquely attributed to those nightside injections.

The fact that the LEGA observations demonstrated the capability of JENI to achieve a continuous survey of a much weaker ENA emitting system, gives us confidence that JENI observations, combined with those by the other PEP ENA imager (Jovian Neutrals Analyzer), will also allow us to identify and disentangle variability components also in a complex system like Jupiter. JENI was able to provide a detailed view of the entirety of the nightside injection events during the LEGA, even (possibly) resolving at the same time finer structures such as LAEs (although this would be discussed in a future analysis), demonstrating its unique capabilities. For example, although previous analyses (e.g. Runov et al., 2011) have shown that the full width at half maximum of injections is rather small (~1 R_E), JENI proved to be capable of imaging the ENA variability of the terrestrial environment continuously from a vantage point of ~17 R_E even up to ~150 R_E. This argues for the expected performance of JENI at the Jovian environment where the scale sizes of important targets are far greater than Earth's, e.g. the Io torus have a diameter of ~12 R_J (1 R_J ~ 69,911km), the Europa gas torus has a diameter of about 25 R_J, whereas Jupiter itself is ~11 R_E.

5 Summary

We employed a set of 7.5-minute accumulation time images of 2.86-85.5 keV Hydrogen ENAs obtained from the JENI detector on board the JUICE spacecraft during the LEGA, to discern substorm dynamics around Earth. During the imaging period, the spacecraft moved away from Earth through ~17 R_E to ~150 R_E, providing images of Hydrogen ENAs from the terrestrial ring current and plasmasheet. The observations are consisted with previous observations of ENAs around Earth, during similar conditions (e.g. IMAGE/HENA) and can be summarized as follows:

- The overall ENA signal strength throughout the 2.86 - 85.5 keV energy range falls off as the spacecraft moves away from the ENA source roughly following a R^{-2} line.
- The rough R^{-2} trend is interrupted by enhancements in ENA emissions, apparent throughout the 2.86 - 85.5 keV energies, which roughly coincide with time periods where the SML index becomes minimum, indicating enhanced substorm auroral activity.
- The nightside ENA emissions around Earth broaden and increase in intensity during each substorm event, whereas the dayside emissions do not show a similar behavior, indicating that the overall ENA morphology around Earth is consistent with transient processes, such as a series of repeated nightside injections and not a global process, such as a global geomagnetic storm, where the Hydrogen ENA intensity would be enhanced nearly symmetrically around Earth, with associated O^+ enhancements in the ring current region.

https://doi.org/10.5194/egusphere-2026-2062
Preprint. Discussion started: 21 April 2026

The ENA images around the substorm events also show clear enhancements at low altitudes, that are possibly indicative of LAEs from plasma sheet injected particles forming the ring current that are charge exchanging and being lost as LAEs. This would be addressed in a future analysis.

Author contributions

The data analysis was performed by KD, MG, PB, DM and ER. KD and MG contributed most of the text. PK and CS contributed to the planning of the PEP-Hi observation sequences. Other co-authors supported the preparation of this article by contributing to the text, reviewing and commenting on the results.

Competing interests

At least one for the (co-)authors is a member of the editorial board of Annales Geophysicae.

Acknowledgements

This work was performed under NASA Task Order 80MSFC23F0077 under Contract 80MSFC20D0004 (ARDES II). JUICE is a mission under ESA leadership with contributions from its Member States, NASA, JAXA, and the Israel Space Agency. It is the first Large-class mission in ESA's Cosmic Vision programme. For the generation of the trajectory plot and the analysis of the geometry of observations we used a series of tools available at https://gitlab.gwdg.de/juice. ER is supported by the German Federal Ministry for Economic Affairs and Climate Action/German Federal Ministry of Research, Technology and Space (BMFTR) through the German Space Agency at DLR on the basis of a resolution of the German Bundestag (Funding codes: 50QJ1301, 50QJ1503 and 50QJ2303) and by the Max Planck Society". NA acknowledges the support of CNES for the Juice mission.

Data availability

The JENI data acquired during the JUICE Moon-Earth flyby in August 2024 are currently under the mission's cruise-phase proprietary period. These data will be made available through the ESA Planetary Science Archive following the first Cruise Archive Delivery, which is currently scheduled for six months after Earth Gravity Assist #3 in 2029.

https://doi.org/10.5194/egusphere-2026-2062
Preprint. Discussion started: 21 April 2026

References

Barabash, S., Lundin, R., Andersson, H., Brinkfeldt, K., Grigoriev, A., Gunell, H., et al. (2006). The Analyzer of Space Plasmas and Energetic Atoms (ASPERA-3) for the Mars Express mission. Space Science Reviews, 126(1-4), 113–164. http://dx.doi.org/10.1007/s11214-006-9124-8

Barabash, S., Sauvaud, J. A., Gunell, H., Andersson, H., Grigoriev, A., Brinkfeldt, K., et al. (2007). The Analyser of Space Plasmas and Energetic Atoms (ASPERA-4) for the Venus Express mission. Planetary and Space Science, 55(12), 1772–1792. http://dx.doi.org/10.1016/j.pss.2007.01.014

Brandt, P. C., Barabash, S., Norberg, O., Lundin, R., Roelof, E. C., Chase, C. J., et al. (1997). ENA imaging from the Swedish micro satellite Astrid during the magnetic storm of 8 February, 1995. Advances in Space Research, 20(4-5), 1061–1066. http://dx.doi.org/10.1016/S0273-1177(97)00561-9

Brandt, Pontus, Stas Barabash, Edmond C. Roelof, and Christopher J. Chase. 2001. 'Energetic neutral atom imaging at low altitudes from the Swedish microsatellite Astrid: Extraction of the equatorial ion distribution', Journal of Geophysical Research: Space Physics, 10.1029/2000ja900023, http://dx.doi.org/10.1029/2000ja900023, 106: 25731-44.

Brandt, P. C., R. DeMajistre, E. C. Roelof, D. G. Mitchell, and S. Mende (2002) IMAGE/HENA: Global ENA imaging of the plasmasheet and ring current during substorms, J. Geophys. Res., 107 (A12), 1454, doi:10.1029/2002JA009307.

Brandt, P. C., Paranicas, C. P., Carbary, J. F., Mitchell, D. G., Mauk, B. H., and Krimigis, S. M. (2008). Understanding the global evolution of Saturn's ring current. Geophysical Research Letters, 35(17). http://dx.doi.org/10.1029/2008gl034969.

Brandt, P. C., Khurana, K. K., Mitchell, D. G., Sergis, N., Dialynas, K., Carbary, J. F., et al. (2010). Saturn's periodic magnetic field perturbations caused by a rotating partial ring current. Geophysical Research Letters, 37(22). http://dx.doi.org/10.1029/2010gl045285

Brandt, P. C., Dialynas, K., Dandouras, I., Mitchell, D. G. Garnier, P., and Krimigis, S. M. (2012). The distribution of Titan's high-altitude (out to 50,000km) exosphere from energetic neutral atom (ENA) measurements by Cassini/INCA. Planetary and Space Science, 60(1), 107–114. http://dx.doi.org/10.1016/j.pss.2011.04.014.

Brandt, P. C., Hsieh, S. Y., DeMajistre, R., and Mitchell, D. G. (2018). ENA Imaging of planetary ring currents. In A. Keiling, O. Marghitu, and M. Wheatland (Eds.), Electric Currents in Geospace and Beyond, Geophysical Monograph Series (Vol. 235, pp. 93–114). American Geophysical Union, Washington, DC. http://dx.doi.org/10.1002/9781119324522.ch6.

Brandt, P. C., 2021, Global Energetic Neutral Atom (ENA) Imaging of Magnetospheres, Space Physics and Aeronomy Collection Volume 2: Magnetospheres in the Solar System, Geophysical Monograph 259, First Edition. Edited by Romain Maggiolo, Nicolas André, Hiroshi Hasegawa, and Daniel T. Welling. © 2021 American Geophysical Union. Published 2021 by John Wiley & Sons, Inc. DOI: 10.1002/9781119815624.ch42

https://doi.org/10.5194/egusphere-2026-2062
Preprint. Discussion started: 21 April 2026

Brandt, Pontus C., Romina Nikoukar, Robert DeMajistre, Robert C. Allen, Donald G. Mitchell, Edmond C. Roelof, Malamati Gkioulidou, and Charles W. Parker. 2022. 'Chapter 2 - Energetic neutral atom imaging of the terrestrial global magnetosphere.' in Yaireska Colado-Vega, Dennis Gallagher, Harald Frey and Simon Wing (eds.), *Understanding the Space Environment through Global Measurements* (Elsevier).

Brandt, P. C., George Clark, Donald G. Mitchell, Peter Kollmann, Matina Gkioulidou, Leonardo Regoli, Kostas Dialynas, Frederic Allegrini, Nicolas Andre, Xianzhe Jia, Krishan Khurana, Carol Paty, Stanislav Barabash, Peter Wurz,In-Situ and Remote Observations of the Radiation Belt and Ring Current during JUICE Lunar Earth Gravity Assist, this journal, Submitted.

Burch, J. L., Moore, T.E., Torbert, R.B. *et al.* Magnetospheric Multiscale Overview and Science Objectives. *Space Sci Rev* **199**, 5–21 (2016). https://doi.org/10.1007/s11214-015-0164-9.

Daglis, I. A. (1997), The role of magnetosphere-ionosphere coupling in magnetic storm dynamics, in Magnetic Storms, edited by B. T. Tsurutani, W. D. Gonzalez, Y. Kamide, and J. K. Arballo, pp. 107-116, American Geophysical Union, Washington, DC.

Daglis, I. A., G. Kasotakis, E. T. Sarris, Y. Kamide, S. Livi, and B. Wilken (1999), Variations of the ion composition during a large magnetic storm and their consequences, Phys. Chem. Earth, 24, 229-232.

DeMajistre, R., E. C. Roelof, P. C. Brandt, and D. G. Mitchell. 2004. 'Retrieval of global magnetospheric ion distributions from high-energy neutral atom measurements made by the IMAGE/HENA instrument', Journal of Geophysical Research: Space Physics (1978–2012), 10.1029/2003ja010322, http://dx.doi.org/10.1029/2003ja010322, 109.

Dialynas, K., S. M. Krimigis, D. G. Mitchell, D. C. Hamilton, N. Krupp, and P. C. Brandt (2009), Energetic ion spectral characteristics in the Saturnian magnetosphere using Cassini/MIMI measurements, J. Geophys. Res., 114, A01212, doi:10.1029/2008JA013761.

Dialynas, K., Brandt, P. C., Krimigis, S. M., Mitchell, D. G., Hamilton, D. C., Krupp, N., and Rymer, A. M. (2013). The extended Saturnian neutral cloud as revealed by global ENA simulations using Cassini/MIMI measurements. Journal of Geophysical Research: Space Physics, 118(6), 3027–3041. http://dx.doi.org/10.1002/jgra.50295

Gkioulidou, M., A. Y.Ukhorskiy, D. G.Mitchell, and L. J.Lanzerotti (2016), Storm time dynamics of ring current protons: Implications for the long-term energy budget in the inner magnetosphere, Geophys. Res. Lett., 43, 4736–4744, doi:10.1002/2016GL068013.

Gkioulidou, M., Clark, G.B., Mitchell, D.G. et al. The IMAP-Ultra Energetic Neutral Atom (ENA) Imager. Space Sci Rev 222, 4 (2026). https://doi.org/10.1007/s11214-025-01256-5

Goldstein, J., K. LLera, D. J. McComas, J. Redfern, and P. W. Valek. 2018. 'Empirical Characterization of Low-Altitude Ion Flux Derived from TWINS', Journal of Geophysical Research (Space Physics), 10.1029/2017ja024957, https://ui.adsabs.harvard.edu/abs/2018JGRA..123.3672G, 123: 3672.

https://doi.org/10.5194/egusphere-2026-2062
Preprint. Discussion started: 21 April 2026

Keesee, A. M., Buzulukova, N., Mouikis, C., & Scime, E. E. (2021). Mesoscale structures in Earth's magnetotail observed using energetic neutral atom imaging. Geophysical Research Letters, 48, e2020GL091467. https://doi.org/10.1029/2020GL091467

Krimigis, S., Mitchell, D., Hamilton, D. et al. A nebula of gases from Io surrounding Jupiter. Nature 415, 994–996 (2002). https://doi.org/10.1038/415994a

Krimigis, S. M., D. G. Mitchell, D. C. Hamilton, S. Livi, J. Dandouras, S. Jaskulek, T. P. Armstrong, J. D. Boldt, A. F. Cheng, G. Gloeckler, J. R. Hayes, K. C. Hsieh, W. -H. Ip, E. P. Keath, E. Kirsch, N. Krupp, L. J. Lanzerotti, R. Lundgren, B. H. Mauk, R. W. McEntire, E. C. Roelof, C. E. Schlemm, B. E. Tossman, B. Wilken, and D. J. Williams. 2004. 'Magnetosphere Imaging Instrument (MIMI) on the Cassini Mission to Saturn/Titan', *Space Science Reviews*, https://ui.adsabs.harvard.edu/abs/2004SSRv..114..233K, 114: 233-329.

Liou, K., Meng, C. I., Lui, A. T. Y., Newell, P. T., and Anderson, R. R. (2000). Auroral kilometric radiation at substorm onset. Journal of Geophysical Research: Space Physics, 105(A11), 25325–25331. http://dx.doi.org/10.1029/2000JA000038.

Mackler, D. A., J.-M.Jahn, J. D.Perez, C. J.Pollock, and P. W.Valek (2016), Statistical correlation of low-altitude ENA emissions with geomagnetic activity from IMAGE/MENA observations, J. Geophys. Res. Space Physics, 121, 2046–2066, doi:10.1002/2015JA021545.

Mauk, B. H., Mitchell, D. G., Krimigis, S. M., Roelof, E. C., and Paranicas, C. P. (2003). Energetic neutral atoms from a trans-Europa gas torus at Jupiter. Nature, 421(6926), 920. http://dx.doi.org/10.1038/nature01431.

Mauk, B. H., Mitchell, D. G., McEntire, R. W., Paranicas, C. P., Roelof, E. C., Williams, D. J., et al. (2004). Energetic ion characteristics and neutral gas interactions in Jupiter's magnetosphere. Journal of Geophysical Research: Space Physics (1978–2012), 109(A9). http://dx.doi.org/10.1029/2003JA010270.

McComas, D.J., Allegrini, F., Baldonado, J. et al. The Two Wide-angle Imaging Neutral-atom Spectrometers (TWINS) NASA Mission-of-Opportunity. Space Sci Rev 142, 157–231 (2009). https://doi.org/10.1007/s11214-008-9467-4.

Mitchell, D., Jaskulek, S., Schlemm, C. et al. High energy neutral atom (hena) imager for the IMAGE mission. Space Science Reviews 91, 67–112 (2000). https://doi.org/10.1023/A:1005207308094.

Mitchell, D. G., P. C. Brandt, E. C. Roelof, D. C. Hamilton, K. C. Retterer, and S. Mende (2003), Global imaging of O+ from IMAGE/HENA, Space Sci. Rev., 109, 63-75

Mitchell, D. G., C. P. Paranicas, B. H. Mauk, E. C. Roelof, and S. M. Krimigis (2004), Energetic neutral atoms from Jupiter measured with the Cassini magnetospheric imaging instrument: Time dependence and composition, J. Geophys. Res., 109, A09S11, doi:10.1029/2003JA010120.

Mitchell, D. G., et al. (2005b), Energetic ion acceleration in Saturn's magetosphere: Substorms on Saturn?, Geophys. Res. Lett., 32, L20S01, doi:10.1029/2005GL022647.

https://doi.org/10.5194/egusphere-2026-2062
Preprint. Discussion started: 21 April 2026

Mitchell, D. G., P. C. Brandt, J. H. Westlake, S. E. Jaskulek, G. B. Andrews, and K. S. Nelson (2016), Energetic particle imaging: The evolution of techniques in imaging high-energy neutral atom emissions, J. Geophys. Res. Space Physics, 121, 8804–8820, doi:10.1002/2016JA022586.

Newell, P. T., and J. W. Gjerloev (2011), Evaluation of SuperMAG auroral electrojet indices as indicators of substorms and auroral power, J. Geophys. Res., 116, A12211, doi:10.1029/2011JA016779.

Nosé, M., Koshiishi, H., Matsumoto, H., Brandt, C. P., Keika, K., Koga, K., et al. (2010). Magnetic field dipolarization in the deep inner magnetosphere and its role in development of O+-rich ring current. Journal of Geophysical Research: Space Physics (1978–2012), 115(A9). http://dx.doi.org/10.1029/2010ja015321

Orsini, S., Livi, S., Torkar, K., Barabash, S., et al. (2010). SERENA: A suite of four instruments (ELENA, STROFIO, PICAM and MIPA) on board BepiColombo-MPO for particle detection in the Hermean environment. Planetary and Space, 58(1-2), 166–181. https://www.sciencedirect.com/science/article/pii/S003206330800278X

Roelof, E. C., Mitchell, D. G., and Williams, D. J. (1985). Energetic neutral atoms (E 50 keV) from the ring current: IMP 7/8 and ISEE 1. Journal of Geophysical Research: Space Physics, 90(A11), 10991–11008. http://dx.doi.org/10.1029/JA090iA11p10991

Roelof, E. C., "Remote Sensing of the Ring Current Using Energetic Neutral Atoms," Adv. Space Res. 9(12), 195–203 (1989).

Roelof, E. C. 1997. 'ENA emission from nearly-mirroring magnetospheric ions interacting with the exosphere', *Advances in Space Research*, 10.1016/s0273-1177(97)00692-3, http://dx.doi.org/10.1016/s0273-1177(97)00692-3, 20: 361-66.

Roelof, Edmond C., and Andrew J. Skinner. 2000. 'Extraction of ion distributions from magnetospheric ENA and EUV images', Space Science Reviews, 10.1023/a:1005281424449, http://dx.doi.org/10.1023/a:1005281424449, 91: 437-59.

Runov, A., Angelopoulos, V., Zhou, X. Z., Zhang, X.J., Li, S., Plaschke, F., and Bonnell, J. (2011). A THEMIS multicase study of dipolarization fronts in the magnetotail plasma sheet. Journal of Geophysical Research: Space Physics (1978–2012), 116(A5). http://dx.doi.org/10.1029/2010ja016316.

Zhao, H., R. H. W. Friedel, Y. Chen, G. D. Reeves, D. N. Baker, X. Li, A. N. Jaynes, S. G. Kanekal, S. G. Claudepierre, J. F. Fennell, J. B. Blake, and H. E. Spence. 2018. 'An Empirical Model of Radiation Belt Electron Pitch Angle Distributions Based On Van Allen Probes Measurements', *Journal of Geophysical Research: Space Physics*, https://doi.org/10.1029/2018JA025277, https://agupubs.onlinelibrary.wiley.com/doi/abs/10.1029/2018JA025277, 123: 3493-511.